

Document downloaded from:

<http://hdl.handle.net/10251/159352>

This paper must be cited as:

Llopis-Albert, C.; Rubio Montoya, F.J.; Valero Chuliá, F.J.; Liao, H.; Zeng, S. (2019). Stochastic inverse finite element modeling for characterization of heterogeneous material properties. *Materials Research Express*. 6(11):1-16.
<https://doi.org/10.1088/2053-1591/ab4c72>



The final publication is available at

<https://doi.org/10.1088/2053-1591/ab4c72>

Copyright IOP Publishing

Additional Information

ACCEPTED MANUSCRIPT

Stochastic inverse finite element modeling for characterization of heterogeneous material properties

To cite this article before publication: Carlos Llopis-Albert *et al* 2019 *Mater. Res. Express* in press <https://doi.org/10.1088/2053-1591/ab4c72>

Manuscript version: Accepted Manuscript

Accepted Manuscript is “the version of the article accepted for publication including all changes made as a result of the peer review process, and which may also include the addition to the article by IOP Publishing of a header, an article ID, a cover sheet and/or an ‘Accepted Manuscript’ watermark, but excluding any other editing, typesetting or other changes made by IOP Publishing and/or its licensors”

This Accepted Manuscript is © 2019 IOP Publishing Ltd.

During the embargo period (the 12 month period from the publication of the Version of Record of this article), the Accepted Manuscript is fully protected by copyright and cannot be reused or reposted elsewhere.

As the Version of Record of this article is going to be / has been published on a subscription basis, this Accepted Manuscript is available for reuse under a CC BY-NC-ND 3.0 licence after the 12 month embargo period.

After the embargo period, everyone is permitted to use copy and redistribute this article for non-commercial purposes only, provided that they adhere to all the terms of the licence <https://creativecommons.org/licenses/by-nc-nd/3.0>

Although reasonable endeavours have been taken to obtain all necessary permissions from third parties to include their copyrighted content within this article, their full citation and copyright line may not be present in this Accepted Manuscript version. Before using any content from this article, please refer to the Version of Record on IOPscience once published for full citation and copyright details, as permissions will likely be required. All third party content is fully copyright protected, unless specifically stated otherwise in the figure caption in the Version of Record.

View the [article online](#) for updates and enhancements.

Stochastic inverse finite element modeling for characterization of heterogeneous material properties

Carlos Llopis-Albert¹, Francisco Rubio¹, Francisco Valero¹, Hunchang Liao², Shouzhen Zeng³

¹Centro de Investigación en Ingeniería Mecánica (CIIM). Universitat Politècnica de València – Camino de Vera s/n, 46022 – Valencia, Spain; Emails: cllopisa@upvnet.upv.es; frubio@mcm.upv.es; fvalero@mcm.upv.es

²Sichuan University, Chengdu, Sichuan 610065, China; Email: liaohuchang@163.com

³Ningbo University, Ningbo 315211, China; Email: zszxl@163.com

Abstract

The micro and meso-structural characteristics of materials present an inherent variability because of the intrinsic scatter in raw material and manufacturing processes. This problem is exacerbated in highly heterogeneous materials, which shows significant uncertainties in the macroscale material properties. Therefore, providing optimal designs and reliable structural analyses strongly depend on the selection of the underlying material property models. This paper is intended to provide insight into such a dependence by means of a stochastic inverse model based on an iterative optimization process depending only of one parameter, thus avoiding complex parametrizations. It relies on non-linear combinations of material property realizations with a defined spatial structure for constraining stochastic simulations to data within the framework of a Finite Element approach. In this way, the procedure gradually deforms unconditional material property realizations to approximate the reproduction of information including mechanical parameters (such as Young's modulus and Poisson's ratio fields) and variables (e.g., stress and strain fields). It allows dealing with non-multiGaussian structures for the spatial structure of the material property realizations, thus allowing to reproduce the coalescence and connectivity among phases and existing crack patterns that often take place in composite materials, being these features crucial in order to obtain more reliable safety factors and fatigue life predictions. The methodology has been successfully applied for the characterization of a complex case study, where an uncertainty assessment has been carried out by means of multiple equally likely realizations.

Keywords: Inverse modelling; Finite Element Method; composite materials; heterogeneity; uncertainty

1. Introduction.

Heterogeneous materials have gained increasing attention in recent years because of its many engineering applications, for instance, in structural and biomechanics problems (e.g., Lloyd et al., 2015; Samavati et al., 2015). Classical examples are metal alloy systems, polymer blends, porous and cracked media, polycrystalline materials and disordered composite materials. However, highly heterogenous materials exhibit spatial and temporal variability in the micro and meso-structural characteristics, which are translated into large uncertainties in their macroscale material properties (Wu and Zhu, 2017). This is due to the intrinsic scatter in raw material, manufacturing processes and external factors during their lifetime.

1
2
3 Heterogeneous materials may entail domain areas with drastic strength differences, which are
4 produced by microstructural heterogeneity, crystal structure heterogeneity or compositional
5 heterogeneity (Khan et al., 2019; Baby et al., 2019; Mikdam et al., 2013; Ni and Chiang, 2007;
6 Kouznetsova et al., 2001). In fact, there are stretchable heterogeneous composites with
7 mechanical gradients with extreme soft-to-hard transitions and with local elastic moduli
8 changes with up to five orders of magnitude (Wu and Zhu, 2017). For example, the biological
9 tissue that connects tendons to bone presents local values of the Young's modulus that can
10 differ by as much as two orders of magnitude to match the stiff surface of bone with the soft
11 tendon. Heterogeneous materials with elastic moduli varying over several orders of magnitude
12 can be manufactured by tuning the local reinforcement of an entangled continuous polymer
13 matrix using reinforcing elements at multiple hierarchical levels (Libanori et al., 2012). In this
14 sense, highly heterogeneous materials do not follow a periodic pattern (i.e., they follow a non-
15 regular microstructural composition), which hampers the achievement of reliable mechanical
16 results. Then the prediction of heterogeneous material properties is becoming a major problem
17 in cases with complex microstructures and multiphase materials (Sharifi et al., 2014). A general
18 constitutive behaviour of material properties can be found in Saabye-Ottosen and Ristinmaa
19 (2005).
20
21
22

23 Another consideration to take into account is the significant differences in the behaviour of
24 materials between the plastic and elastic regimes. Consequently, the challenge in using
25 heterogeneous materials range from material design, material property predictions, to use limit
26 and lifetime predictions (Torquato, 2010). The problem is compounded by the difficulty in
27 obtaining the material properties either because of the economic cost and time-consuming of
28 establish them experimentally or by technical impediments. Several efforts have been carried
29 out to circumvent the problem of data acquisition, which are based on two main approaches.
30 The first approach considers the morphology and constitutive characteristics of the material at
31 the microscale as random entities. Then, stochastic homogenisation techniques are applied to
32 determine the macroscale properties of the material (Sakata et al., 2008). Nevertheless, this
33 approach is hampered by the fact that gathering high-quality and sufficient data at this scale is
34 not always feasible. The second approach is based on direct measurements at the macroscale
35 material properties. Readers are referred to other papers for more comprehensive reviews on
36 the uncertainty representation of material properties (Charnpis et al., 2007; Sriramula and
37 Chryssanthopoulos 2009).
38
39
40

41 There is a wide range of techniques for the measurement of material properties, such as
42 extensometers, photoelasticity. For instance, the Digital Image Correlation (DIC) and Digital
43 Volume Correlation (DVC) are gaining growing interest because their ability to non-destructively
44 access internal strains in materials (Cooreman et al., 2008; Li et al., 2014; Mortazavi et al., 2014;
45 Kashfi et al., 2017; 2018; Majzoubi et al., 2018). That is, they provide full displacement and strain
46 measurements fields on the surface, including inside opaque materials when subjected to
47 external loadings. These optical non-contact methods provide a great amount of experimental
48 data that has bring about the proliferation of inverse methods for material characterisation (e.g.,
49 Li et al., 2014 Kim et al., 2015). The accuracy of these approaches has been widely treated in the
50 literature (Cooreman et al., 2008). Furthermore, these techniques can be applied to both
51 macroscopic and microscopic scales. The experimental information obtained with these
52 approaches can be implemented in numerical models for analysis and design of heterogeneous
53 materials. They require an accurate representation of the relevant physics and their interactions
54 and a quantitative assessment of underlying uncertainties and their influence on design
55 performance targets. Therefore, the reliability in such models depends on the choice of the
56 underlying material property.
57
58
59
60

Several attempts for modelling the effects of the heterogeneity on the mechanical response has been reported in the literature (e.g., Zottis et al., 2018; Zhang et al., 2018; Albanesi et al., 2018; Borkowski and Kumar 2018; Albanesi et al., 2017; Chakraborty and Eisenlohr, 2017; Goodarzi et al., 2016; Borovinšek et al., 2016; Herrera-Solaz et al., 2015; Fu et al., 2013; Ramani et al., 2013; Mehrez et al., 2012; Mehrez et al., 2012a; Pottier et al., 2011). These optimization techniques provide a systematic means of designing materials with tailored properties for a specific application. This is performed by data assimilation to identify stochastic structures of uncertain mechanical parameters. There are many successful applications in the fields of inverse problems such as non-destructive testing and characterization of material properties by ultrasonic or X-ray techniques, thermography, etc. Generally speaking, the inverse problems are concerned with the determination of the input and the characteristics of a mechanical system from some of the output from the system. Mathematically, such problems are ill-posed and have to be overcome through development of new computational schemes, regularization techniques, objective functionals, and experimental procedures. These methodologies are used to characterize the properties of a wide range of heterogeneous materials, including composite materials, porous media, colloidal dispersions, concrete mixtures, ceramics, metallic alloys and polymer blends (e.g., Ignacio 2014; Pitangueira and Silva, 2002).

This paper is concerned with the uncertainty representation of highly heterogeneous materials. The objective is to characterise macroscopic material properties of heterogeneous materials from scarce macroscale experimental measurements. This is achieved by means of a stochastic inverse model, which allows to optimize the structure and macroscopic properties of heterogeneous materials. It can be applied to composite materials, but also could be applied to porous media, colloidal dispersions, and polymer blends. This powerful tool is embedded into a FE framework and presents several advantages with regard to already existing techniques as explained in the next section. The basic principle is to iteratively minimize a penalty function which expresses the discrepancy between the experimentally measured and the numerically computed response of the physical system under study. Therefore, the unknown set of parameters of the composite constituents are iteratively tuned so as to match experimental and computed values as closely as possible. The methodology can deal with both random uncertainties, on account of sample inter-variabilities, and epistemic uncertainties because of scarce availability of data. It has been successfully applied to a case study, while providing an uncertainty assessment and reduction for the optimal design of highly heterogeneous materials.

2. Materials and methods.

2.1. Stochastic structure and generation of material properties fields.

The prediction of mechanical properties (elastic constants) of elastic heterogeneous materials is performed using a homogenization process, in which the material is idealized as being effectively homogenous in a Representative Volume Element (RVE) at the macroscopic level. This is despite the fact that these materials can be considered as heterogeneous media at the microscopic scale. This simplification is assumed because the high computational cost prevents the use of a fine mesh in numerical models to accurately represent microstructure heterogeneities. Furthermore, common composite material comprises three components: discontinuous or dispersed multiphases, the matrix as the continuous phase, and the fine interface area. Several composites materials with such complex microstructures are found in practice, for example, in biomechanics such as musculoskeletal tissue and bone, porous ceramics, porous scaffolds for tissue engineering, metal-composite joints in automotive and aerospace applications, and biomedical implants in orthopaedics (Ni et al., 2007).

The material properties at the macroscale take into account the properties of all phases belonging to the heterogeneous material and their interaction within the RVE at the microscale.

1
2
3 In this sense, homogeneous values obtained depend on the multiphase structure. This is related
4 to a combination of factors such as the size, random volume percentage of the constituent
5 phases, their geometry and their spatial distribution (i.e., position and orientation), possible
6 defects, and phase coalescence and connectivity inside the RVE. For instance, channels
7 generated by phase connectivity may strongly affect the crack pattern characteristics. Such
8 combination of factors leads to different local material properties, anisotropy (difficult to
9 measure experimentally) and higher or lower heterogeneity.

10
11
12 As a result, the heterogeneity of material properties (e.g., the elastic modulus) and its associated
13 gradients takes an important role to fracture resistance and toughness. It has been
14 demonstrated that gradients in the elastic modulus of a surface can affect the toughness of that
15 surface. So far, several rigorous homogenization processes can be found in the literature (e.g.,
16 Libanori et al., 2012).

17
18
19 The present methodology shares some similarities with the classical homogenization and mixing
20 theories but goes a step further by overcoming some of their limitations and assumptions
21 (Sánchez-Palencia, 1987; Oller, et al. 2005). Moreover, it also overcomes the limitations of
22 analytical and statistical methods. Both methodologies assume the existence of representative
23 volume elements (RVE) with homogenized material properties at the macroscopic level but have
24 important differences.

25 The main difference is that classical homogenization techniques are embedded into a stochastic
26 inverse model in which the heterogeneity at each unsampled RVE is estimated by a local
27 conditional probability distribution function (cpdf) as explained below. Therefore, the
28 methodology can at a certain extent to represent the microscopic (or local) scale
29 heterogeneities.

30
31
32 In this sense the developed methodology, for the purposes of the data analysis and the
33 correlation structure of the material properties, relies on an indicator conditional simulation
34 technique (Gómez-Hernández and Srivastava, 1990). Using this technique, a set of material
35 property realizations, named as seed fields, are generated, which provides stochastic
36 simulations of a variable that honours the material property data. That is, the seed parameter
37 fields are conditional to elastic modulus and Poisson's ratio measurements, and also to
38 secondary data, for instance, from expert judgement. Then, those data are defined into a series
39 of indicators, which allow to estimate the conditional probability distribution function (cpdf) of
40 the studied variable at any unsampled location using indicator kriging algorithms. A detailed
41 explanation of these methodologies can be found in Goovaerts (1997).

42
43
44 These cpdf and the indicator variograms allow defining the a priori stochastic structure of the
45 seed parameter fields. In addition, the indicator variogram also allows to determine the spatial
46 continuity of the upscaled parameter field (e.g., the elastic modulus). Furthermore, the
47 methodology does not require considering for the spatial structure of the material property
48 realizations the classical multi-Gaussian hypothesis, thus allowing to reproduce the coalescence
49 and connectivity among phases and existing crack patterns that often take place in
50 heterogeneous materials, being these features crucial in order to obtain more reliable safety
51 factors and fatigue life predictions. Additionally, the methodology can vary the a priori stochastic
52 structure during the iterative optimization process to constraint simulations to available data,
53 to correct possible errors in the conceptual model and to integrate information not captured by
54 conditioning data.

55
56
57 Using these methodologies, we define a range of variation of the studied variable z , which is
58 discretized into $(K+1)$ categories using K threshold values z_k . We also define \mathbf{u}_α as a datum
59 location; $z(\mathbf{u}_\alpha)$ as a hard datum, which is a precise measurement of the attribute of interest.

Then $i(\mathbf{u}_\alpha; z_k)$ are binary (hard) indicator data. Then the indicator variables are built by comparing measurements $z(\mathbf{u}_\alpha)$ to a set of thresholds, z_k . Then the local prior probabilities are binary indicator data (i) defined as (e.g., Goovaerts, 1997):

$$i(\mathbf{u}_\alpha; z_k) = \begin{cases} 1 & \text{if } z(\mathbf{u}_\alpha) \leq z_k \\ 0 & \text{otherwise} \end{cases} \quad k = 1, \dots, K \quad (1)$$

Subsequently, any new particular simulated value is attained by straightforward MonteCarlo drawing. Eventually, each simulated value is added in the conditioning data set so that the next simulated values at other locations be conditioned to it. This technique has the advantage to impose the bivariate (2-point) statistics on the simulated field instead of defining a simple covariance model.

This technique uses the experimental indicator semiovariogram (γ_I) to perform a data analysis and determine the spatial continuity of the upscaled elastic modulus, i.e., after the homogenisation process of the material properties within the RVE at the macroscopic level where the measurements are taken:

$$\frac{\gamma_I(\mathbf{h}; z_k)}{\sigma_I^2} \approx \frac{1}{2N(\mathbf{h})_{\mathbf{u}_1 - \mathbf{u}_2 = \mathbf{h} \pm \Delta \mathbf{h}}} \sum [i(\mathbf{u}_1; z_k) - i(\mathbf{u}_2; z_k)]^2 \quad (2)$$

where z_k are the thresholds values; σ_I^2 is the indicator variance given as $\sigma_I^2 = F(z_k)[1 - F(z_k)]$, and $F(z_k)$ is the marginal cumulative distribution function; $N(\mathbf{h})$ is the number of data pairs within the class of distance and direction; \mathbf{h} is the separation vector; $z(\mathbf{u}_{1,2})$ represents a measurement, $\mathbf{u}_{1,2}$ is the vector of spatial coordinates of the individual 1 or 2, and $\Delta \mathbf{h}$ is a tolerance vector.

Therefore, the a priori stochastic structure of these seed parameter fields is defined by means of the *cpdf* and the indicator variograms, thus allowing the method to adopt any Random Function (RF) model. Then the methodology does not require considering for the spatial structure of the material property realizations the classical multi-Gaussian hypothesis, thus allowing to reproduce the coalescence and connectivity among phases and existing crack patterns that often take place in heterogeneous materials, being these features crucial in order to obtain more reliable safety factors and fatigue life predictions.

2.2. Stochastic inverse model.

The presented stochastic inverse method is used for the simulation of uncertain mechanical parameter fields (e.g., material properties such as the elastic modulus or Poisson's ratio) conditional to measurements of those parameters and also to stress and strain data. The formulation of the method is based on a modified version of the gradual deformation method for constraining stochastic simulations to data (Hu, 2000). The flowchart of the method is presented in Fig. 1. As a first step, a set of material property realizations, named as seed fields, are generated as explained above.

In the second step, the method performs an iterative optimization procedure based on successive non-linear combinations of seed realizations (Z):

$$Z^m = \alpha_1 Z^{m-1} + \alpha_2 Z_{2m} + \alpha_3 Z_{2m+1} \quad \text{with } Z_0 = Z^1 \quad (3)$$

where subscripts represent seed fields and superscripts stand for conditional fields resulting from a previous non-linear combination. Then, for each iteration m , the field Z^{m-1} , from the

previous iteration, is combined with 2 new independent realizations Z_{2m} and Z_{2m+1} . The method entails combining at least 3 conditional realizations at a time to assure the preservation of mean, variance, variogram and Z data in the non-linearly combined field. Therefore, it preserves not only the first and second order statistics of the experimental samples and approximates their marginal distribution, but also preserves the stochastic structure. A transformation for considering the non-Gaussianity feature is required. This is carried out by means of the probability fields, which lead to non-linear combinations of seed conditional realizations (Capilla and Llopis-Albert 2009). The probability fields are made up through the local *cpdf*, i.e., the probability density function obtained at each element of the discretization using the ensemble values of the seed fields.

The coefficients must also fulfil the constraints in Eq. (4-5) to preserve the model structure during the iterative optimization process, i.e., the preservation of mean, variance, variogram and conditional data in the combined field [Ying and Gómez-Hernández, 2000]. Therefore, all seed fields are generated as equally probable non-multiGaussian realizations and share the same stochastic structure.

$$\begin{cases} \alpha_1 + \alpha_2 + \alpha_3 = 1 \\ (\alpha_1)^2 + (\alpha_2)^2 + (\alpha_3)^2 = 1 \end{cases} \quad (4)$$

where the parameter α_i must also comply with:

$$\begin{cases} \alpha_1 = \frac{1}{3} + \frac{2}{3} \cos \theta \\ \alpha_2 = \frac{1}{3} + \frac{2}{3} \sin(-\frac{\pi}{6} + \theta) \\ \alpha_3 = \frac{1}{3} + \frac{2}{3} \sin(-\frac{\pi}{6} - \theta) \end{cases} \quad \text{with } \theta \in [-\pi, \pi] \quad (5)$$

Each of these spatially variable Young's modulus fields can be considered as independent realisations and equally probable realizations of an underlying continuous Young's modulus random field.

In the third step, a numerical approximation of the stress (σ) and strain (u) fields is obtained using the Finite Element Method (FEM). For that purpose, the capabilities of the commercial Finite Element Analysis (FEA) software ANSYS (Version 18.2, ANSYS Inc.) were used. Therefore, linear and non-linear behaviours of material properties can be analysed. For practical engineering problems the only limitations regarding the constitutive behaviour about how materials respond to various loadings are those imposed by ANSYS. Note that the FEM is the most widely used numerical method for determining the overall mechanical response of heterogeneous materials to given solicitations.

In this way, the procedure gradually deforms the seed material property fields to approximate the reproduction of stress and strain fields within the framework of a finite element approach.

In the fourth step, at each iteration k of the method the parameter θ is obtained by minimizing an objective function that penalizes the difference between measured and computed data. Note that the objective function only depends on one parameter (θ), thus avoiding a complex parametrization that may lead to numerical problems and high computational cost. Then the FEM provides, based on the optimized parameter θ at each iteration of the procedure, the

computed stress (θ) and displacement $u(\theta)$ fields. The penalty function to be minimized consist of the weighted sum of two terms:

$$p^k(\theta) = p_u^k(\theta) + \Phi^k p_\sigma^k(\theta) = \sum_{t=1}^{N_t} \left[\sum_{i=1}^{m_{u,t}} \omega_{u,i,t} (u_{i,t}^m - u_{i,t}(\theta))^2 + \Phi^k \sum_{j=1}^{m_{\sigma,t}} \omega_{\sigma,j,t} (\sigma_{j,t}^m - \sigma_{j,t}(\theta))^2 \right] \quad (6)$$

where $p_\sigma^k(\theta)$ and $p_u^k(\theta)$ are the weighted sum of square deviations among observed and calculated values for stresses and displacements, respectively. They are function of the parameter θ , for every time step t and measurement location i . The term Φ^k is the trade-off coefficient between the conditioning data; k is the iteration number; N_t is the number of time steps with measurements; $m_{u,t}$ and $m_{\sigma,t}$ are number of displacement and stress data at sampling time t , $\omega_{u,j,t}$ and $\omega_{\sigma,i,t}$ stand for weight assigned to the i displacement and j stress measurement, at sampling time t , respectively; $u_{i,t}^m$ and $\sigma_{j,t}^m$ are the measured displacement and stress at time t , while $u_{i,t}$ and $\sigma_{j,t}$ refer to the computed values as a function of parameter θ , at their corresponding sampling locations and times. The weighting coefficients take into account the measurement and estimation errors and can be assigned to modulate the importance of different sampling locations and times, based on expert knowledge or other considerations.

In the step 5 an iteration stop test is performed, which is based on a combination of three criteria: i) the value reached by the objective function; ii) relative decline of the objective function compare to its value in previous iterations; iii) and maximum number of iterations (k_{\max}). When the iterations loop stops, a simulated field Z is achieved, otherwise the methodology proceeds to the next iteration $k = k + 1$, in step 2.

3. Application to a case study.

The inverse model is applied to the prediction of elastic properties of a theoretical heterogeneous material with multiphases and complex microstructures. This is exemplified with a case study involving a bending of a composite beam. A beam of length 4 m, and a height and width of 0.4 m, has been discretized using blocks of 0.1 m, so that the geometry is made up of 640 blocks. Then the domain has been discretized using a RVE consisting of cubes 0.1 m, which are modelled using SOLID185 elements, as defined by ANSYS. The geometry selection tries to balance the computational cost with the size of the RVE to obtain a proper representation of the heterogeneous material.

At each of these blocks, different material properties (i.e., Young's modulus and Poisson's ratio) are assigned. Several boundary conditions are applied. The beam is fixed at one of its ends in all DOF's and on the free-end it is subjected to a bending moment M_y . This is obtained applying a pressure of 1 MPa at the top face of the blocks belonging to the free end.

In order to define the stochastic structure and the spatial continuity for the generation of the material properties a sequential indicator simulation technique is used, as explained above. The seed fields are defined with the same variogram for all indicator categories, except for the extreme ones, which were defined with a 15% more continuity to allow the reproduction of the coalescence and connectivity among phases and existing crack patterns.

A nugget effect of 0.02, a sill of 0.2, and ranges of 8, 4, 4 for the directions X, Y, and Z, respectively, were used. The Young's modulus is defined to vary between 15 and 40 MPa divided into nine categories with their respective thresholds. A similar approach is used for the Poisson's coefficient, which is defined to vary between 0.25 and 0.35. A variogram analysis of the indicator

categories shows that a proper adjustment of the indicator semivariogram to data is achieved using an exponential model:

$$\frac{\gamma_I(\mathbf{h}; z_k)}{\sigma_I^2} = c_0 + c_1 \cdot [1 - \exp(-3\|\mathbf{r}(\mathbf{h})\|)] \quad (7)$$

where c_0 is the nugget, c_1 is the structure sill, and $\mathbf{r}(\mathbf{h})$ is the corresponding separation vector for an equivalent isotropic variogram, which is achieved by orienting the correlation structure along the coordinates and scaling the ranges to unitary values.

With this information, as a first step, an ensemble of 10100 fields -for both the elastic modulus (E) and Poisson's ratio (ν)- are generated using the indicator sequential simulation code ISIM3D (Gómez-Hernández and Srivastava, 1990), but with being conditional to any data. These fields are referred as unconditional fields. One of these fields is chosen as the reference field, where different conditioning data are extracted. Then, as a second step, an ensemble of 10100 seed fields for both material properties are also generated using this technique. Note that since a hundred conditional simulations will be obtained, such large number of seed parameter fields are required. The generated seed fields are equally likely realizations, thus being plausible representations of reality since they display the same degree of spatial variability.

Finally, all this information is implemented in an ANSYS model to obtain the mechanical response of the composite beam problem. Therefore, this mechanical response is computed with a FE approach and the a priori unknown material properties are iteratively updated in such a way that the computed results match the measured fields as closely as possible.

The criterion to assess simulation results is based on the following performance measures, which compare computed values obtained using the FE approach with measurements:

$$\eta_v = \sqrt{\frac{1}{m_v} \sum_{i \in m_v} \omega_{i,v} (v_i - v_i^m)^2} \quad \text{with } v = u \text{ or } v = \sigma \quad (8)$$

The performance measure η_v computed at a given iteration k (having combined a total of $2k+1$ seed fields), is defined as the square root of a weighted mean of the square departures of computed values (v) from the measured values (v^m) after iteration k ; where ω_i are the weights assigned to each type of measurement v_i ($i=1, \dots, m_v$), which are defined to add up to the unity. Additionally, an assessment of the conditional and unconditional fields is carried out based on the average value, $\eta_{v,m}$, and on the standard deviation, $\eta_{v,\sigma}$, of the performance measures defined in Eq. (8).

4. Results and discussion.

The developed methodology is intended to provide a stochastic characterization of a composite material through the analysis of multiple realizations in the framework of an inverse model. Fig. 2 shows the effective parameters for the reference field together with its geometry shared by all seed fields. Fig. 2a depicts the spatial heterogeneity of the elastic modulus for the reference field, while Fig. 2b does the same for the Poisson's ratio. Fig. 2c presents the displacement field, with a maximum value of 0.0156 m. Fig. 2d represents the von Misses stress field, which ranges from 0.072 to 22 MPa. Fig. 3 shows for the reference field the frequency distribution and the univariate statistics of the elastic modulus and Poisson's ratio values. These values clearly show that non-Gaussian parameter fields were generated. Fig. 4 presents the values and spatial

1
2
3 location of conditioning data with regard to the elastic modulus (Fig. 4a), the Poisson's ratio (Fig.
4 4b) and the stress field (Fig. 4c). A total of 76 data are selected as conditioning data for each
5 variable, which are uniformly distributed along the domain.
6

7
8 Fig. 5 illustrates the frequency distribution and the univariate statistics for an ensemble 100
9 fields of both unconditional and conditional fields. It is displayed for both the elastic modulus
10 and Poisson's ratio values. For the conditional field the histogram exhibits a non-Gaussian
11 distribution with a bias to higher and lower values, thus allowing to reproduce strings of extreme
12 effective parameter values. This enables to take into account the coalescence and connectivity
13 among phases and existing crack patterns that often take place in heterogeneous materials,
14 being these features crucial in order to obtain more reliable safety factors and fatigue life
15 predictions.
16

17
18 On the one hand Fig. 6 shows, for an ensemble of a hundred unconditional realizations, both
19 the ensemble mean (μ) and standard deviation (σ) fields. Fig. 6a presents that mean for the
20 elastic modulus (μ_E), while Fig. 5b depicts the standard deviation (σ_E). Fig. 6c and Fig. 6d do the
21 same for the displacement (u) field (i.e., μ_u and σ_u). Again, Fig. 6e and 6f show the same for the
22 von Mises stress ($\mu_{\sigma_{VM}}$, $\sigma_{\sigma_{VM}}$) field. On the other hand, Fig. 7 presents the same results for an
23 ensemble of a hundred conditional realizations.
24

25
26 Fig. 8 depicts for a given conditional realization the material property fields (i.e., elastic modulus
27 and Poisson's ratio), and its corresponding displacement and stress fields. This figure shows how
28 the heterogeneity in the material properties is translated into the displacement and stress fields.
29

30
31 In order to perform a comparison and to highlight the worth of the developed methodology the
32 results of a homogeneous material property field are also provided. It uses the values for all
33 blocks of the discretization of 27.5 MPa for the elastic modulus and 0.3 for the Poisson's ratio.
34 Fig. 9a illustrates for this homogeneous realization the displacement field, while Fig. 9b shows
35 the stress field.
36

37
38 Fig. 10 exhibits the field of deformations for a given realization, i.e., the field of optimal
39 increments added to a certain unconditional field for obtaining a conditional simulation after
40 the conditioning process consisting of $k=50$ iterations. In other words, is the perturbation
41 induced at each element of the discretization of an unconditional parameter field during the
42 iterative optimization process in order to obtain the conditional field. This number of iterations
43 has been considered as adequate based on the convergence behaviour of the penalty function
44 in the inverse model.
45

46
47 Results reveal that conditional simulations of the material heterogeneity shows a good
48 agreement between the estimated effective Young's modulus and Poisson' ratio and their
49 corresponding values in the reference field. Additionally, significant differences can be
50 appreciated between unconditional and conditional fields, which arise as a result of the gradual
51 deformation process performed by the iterative optimization for constraining stochastic
52 simulations to data. The perturbations clearly show that noteworthy changes in the parameter
53 fields are induced (Fig. 10). Moreover, these differences can be observed throughout all the
54 figures comparing unconditional and conditional fields. For instance, when comparing results
55 with regard to those obtained with homogenous parameters fields (Fig. 9). This clearly shows
56 how considering homogeneous parameter fields disregard important material properties
57 features that lead to significant differences in their mechanical response. Also, when comparing
58 Fig. 6a and Fig. 7a, it is clear how the ensemble average field of conditional simulations for the
59 elastic modulus presents a wider range of values to come close to data.
60

1
2
3 Since the elastic modulus measures the degree of stiffness of a material, the inverse model leads
4 to some parts of the domain become much stiffer (i.e., with high Young's modulus), while other
5 parts shift to be more flexible after the deformation process. Therefore, the required loads to
6 elastically deform the mechanical component and alter its shape also change. It is worthwhile
7 mentioning that the degree of stiffness is highly important in designing products which can only
8 be allowed to deflect by a certain amount (e.g., bridges) or, for instance, in springs. They are
9 also important in transport applications, where the stiffness is required at minimum weight, and
10 materials with a large specific stiffness are the most suitable. In addition, the higher continuity
11 for extreme values observed in the conditional fields reinforce the fact of the non-Gaussian
12 feature (Fig. 7).
13
14

15 In this sense, results also illustrates that although the inverse model is intended to preserve the
16 mean, variance, variogram and conditional data in the combined field, it is able to partially
17 modify the stochastic structure to come close to the available data, to correct possible errors in
18 the conceptual model and to integrate information not captured by conditioning data.
19

20
21 Furthermore, the inverse model tends to preserve the local *cpdf's* (i.e., at each RVE of the
22 domain) during the whole perturbation process of seed fields to attain conditional simulations.
23 This can be observed in Fig. 10 and it is triggered by the significant perturbations carried out
24 over the unconditional fields. This means that if there are zones of the domain with *cpdf's*
25 belonging to independent stochastic processes they will be still preserved. Hence, results show
26 the connectivity of high and low values the elastic modulus, which may strongly influence the
27 propagation and coalescence of the crack pattern and the effective fracture toughness. Then
28 the methodology allows to determine local damages in the domain, which are characterize by a
29 reduction in the effective elastic modulus. Furthermore, elastic moduli contrast between
30 adjacent RVE can also significantly alter the effective toughness. The mesh independency is
31 validated by the fact that the solution does not vary significantly even if the mesh is further
32 refined, i.e., we have proved that the percentage difference between two successive meshes is
33 negligible at the macroscale of the representative volume elements (RVE). Of course, a very fine
34 mesh could lead to different results, but the computational cost would prevent the use of such
35 mesh.
36
37
38

39 On the one hand, it can be also concluded when comparing unconditional and conditional fields
40 that a significant reduction of uncertainty is achieved, as shown in Fig. 6b and Fig. 7b. The
41 standard deviation values of the conditional realizations for the elastic modulus present a drastic
42 reduction. The values are zero in the spatial location of data, and near to zero in their vicinity.
43 This fact leads to more reliable material properties estimation, which is translated into a
44 valuable knowledge on the full-field displacements and stresses. However, a lower uncertainty
45 reduction is attained for the ensemble displacement and von Mises fields (Fig. 6d and Fig. 7d,
46 and Fig. 6f and Fig. 7f).
47

48 On the other hand, the ensemble average differences between the unconditional and
49 conditional fields present a different behaviour. That is, the ensemble average difference for all
50 blocks of the domain is 4.2 MPa for the Young's modulus field, 0.016 for the Poisson's ratio,
51 1.46E-04 m for the displacement and 0.30 MPa for the von Mises stress.
52

53 Then differences for the elastic modulus (Fig. 6a and Fig. 7a) are remarkable but on the contrary
54 the displacement and von Mises stress fields are hardly affected by the iterative optimization
55 process. This does not mean the non-existence of changes during the conditioning procedure
56 for a certain conditional field, instead it is because both unconditional and conditional
57 simulations share the same stochastic structure (same variography), boundary conditions,
58 geometry definitions, and are modelled with the same discretization and element type.
59
60

The maximum values considering all RVE of the domain also differ for the unconditional and conditional fields. The mean of the maximum values for the displacement of all unconditional fields is 1.46E-02 m, while the standard deviation of these maximum values is 9.95E-04 m. For the conditional fields is 1.45E-02 m, while the standard deviation is 2.61E-04 m. With regard to the von Mises stress for the unconditional fields the mean of the maximum values is 1.6E+07 Pa, while the standard deviation is 7.74E+05 Pa. For the conditional fields is 1.57E+07 Pa, while the standard deviation is 5.62E+05 Pa. Obviously, the maximum values take place at different spatial locations for the different realizations.

Finally, Table 1 shows the performance measurements of the first unconditional and conditional field for both displacements η_u and von Mises stresses $\eta_{\sigma_{VM}}$. Likewise, this table also presents, for the ensemble average of unconditional and conditional fields, the values of $\eta_{u,m}$ and $\eta_{\sigma_{VM},m}$. These results are obtained after 50 iterations of the inverse model and using a set of a hundred unconditional and conditional realizations. These values show a good agreement between computed and measured values. Furthermore, important reductions regarding the reference field in percentage terms are achieved. Regarding the mesh convergence results have shown that very few iterations are required since the problem is relatively linear. This proves the worth of the presented methodology and the appropriateness of conditioning to as much information as possible to reduce the uncertainty in the mechanical predictions.

Table 1. Performance measurements of the first unconditional and conditional field for both displacements η_u and von Mises stresses $\eta_{\sigma_{VM}}$. Likewise, for the ensemble average of the unconditional and conditional fields ($\eta_{u,m}$, $\eta_{\sigma_{VM},m}$). In parenthesis is presented the percentage reduction of η regarding the reference field.

	η_u [m]	$\eta_{u,m}$ [m]	$\eta_{\sigma_{VM}}$ [MPa]	$\eta_{\sigma_{VM},m}$ [MPa]
Unconditional fields	3.96E-09	5.88E-09	29.8	23.55
Conditional fields	1.44E-09 (63.63%)	1.34E-09 (77.21%)	16.47 (44.73%)	12.38 (47.43%)

Note, that because of the few available data the a priori stochastic structure presents a high uncertainty. Therefore, a higher performance of the stochastic inverse model should be expected when more data were available, or a fine discretization was used. On the contrary, higher differences between unconditional and conditional realizations and lower reduction of the penalty function would be achieved if a wider range of material properties would have been selected or the unconditional fields would have been generated with different stochastic structure. Finally, the major limitation in the developed methodology is the difficulty in the conceptual definition of the a priori stochastic structure of seed parameter fields, which is defined by means of the local conditional probability distribution function (cpdf) and the indicator variograms. A wrong structure definition may lead to long computational times, i.e., many iterations would be needed to gradually change the a priori stochastic structure during iterative optimization process to constrain simulations to data. This process allows to come close to available data, to correct possible errors in the conceptual model and to integrate information not captured by conditioning data.

5. Conclusions.

This article presents a stochastic inverse model for accurately computing effective material properties of heterogeneous materials with both intermingled and randomly dispersed multiphases. In this way the fully automated numerical tool optimizes the structure and macroscopic properties of heterogeneous materials by identifying a selected set of unknown material parameters. This is carried out by means of on non-linear combinations of material property realizations with a defined spatial structure for constraining stochastic simulations to data within the framework of a Finite Element approach.

The methodology can be applied for the characterization and to the optimal design of heterogeneous materials, for instance, to better determine its degree of stiffness. The unknown material parameters in the finite element model are iteratively tuned so as to match the experimentally measured and the numerically computed variables as closely as possible. In this way, the inverse model allows characterising macroscopic material properties of highly heterogeneous materials from limited macroscale experimental measurements. Then it allows determining, in an accurate way, key structural parameters such as the effective modulus of elasticity and the Poisson's ratio and the corresponding mechanical response. Therefore, it can help designers to properly analyse the effect of heterogeneity on fracture-damage behaviour and fatigue lifetime. As a result, it can reduce designing times and financial costs. In addition, the inverse material characterization does not require full-field measurement data on the whole domain and, thus leading to a computational efficient algorithm. Furthermore, the iterative optimization process presents important advantages and depends only of one parameter, thus avoiding a complex parametrization, numerical problems and high computational cost. In addition, because of using a FE approach, problems with complex geometries and boundary conditions can be efficiently analysed.

The methodology has been successfully applied to a case study and includes an uncertainty assessment by means of Monte Carlo simulations, and the results have been obtained in a non-multiGaussian framework.

References

- Albanesi, A., F. Bre, V. Fachinotti, C. Gebhardt (2018). Simultaneous ply-order, ply-number and ply-drop optimization of laminate wind turbine blades using the inverse finite element method. *Composite Structures* 184, 894-903.
- Albanesi, A., V. Fachinotti, I. Peralta, B. Storti, C. Gebhardt (2017). Application of the inverse finite element method to design wind turbine blades. *Composite Structures* 161, 160-172.
- Borkowski, L., R.S. Kumar (2018). Inverse method for estimation of composite kink-band toughness from open-hole compression strength data. *Composite Structures* 186, 183-192.
- Baby, A., Nayak, S., Heckadka, S., Purohit, S., Bhagat, K., Thomas, L. (2019). Mechanical and morphological characterization of carbonized egg-shell fillers/Borassus fibre reinforced polyester hybrid composites. *Materials Research Express* 6(10), 105342. DOI: 10.1088/2053-1591/ab3bb7.
- Borovinšek, M., M. Vesenjak, Z. Ren (2016). Estimating the base material properties of sintered metallic hollow spheres by inverse engineering procedure. *Mechanics of Materials* 100, 22-30.
- Capilla, J.E., C. Llopis-Albert (2009). Stochastic inverse modeling of non multiGaussian transmissivity fields conditional to flow, mass transport and secondary data. 1 Theory. *Journal of Hydrology* 371, 66-74.
- Chakraborty, A., P. Eisenlohr (2017). Evaluation of an inverse methodology for estimating constitutive parameters in face-centered cubic materials from single crystal indentations. *European Journal of Mechanics - A/Solids* 66, 114-124.

- 1
2
3 -Charpis, D. C., G. I. Schueller, M. F. Pellissetti (2007). The need for linking micromechanics of
4 materials with stochastic finite elements: A challenge for materials science. *Computational*
5 *Materials Science* 41(1), 27–37.
- 6 -Cooreman, S., D. Lecompte, H. Sol, J. Vantomme, D. Debruyne (2008). Identification of
7 Mechanical Material Behavior Through Inverse Modeling and DIC. *Experimental Mechanics* 48,
8 421–433.
- 9 -Fu, Y.Z., Z.R. Lu, J.K. Liu (2013). Damage identification in plates using finite element model
10 updating in time domain. *Journal of Sound and Vibration* 332, 7018–7032.
- 11 -Gómez-Hernández, J.J., R.M. Srivastava, (1990). ISIM3D: an ANSI-C three dimensional multiple
12 indicator conditional simulation program. *Computer Geoscience* 16(4), 395–440.
- 13 -Goodarzi, A., M. Fotouhi, H.M. Shodja (2016). Inverse scattering problem of reconstruction of
14 an embedded micro-/nano-size scatterer within couple stress theory with micro inertia.
15 *Mechanics of Materials* 103, 123-134.
- 16 -Goovaerts, P. (1997). *Geostatistics for Natural Resources Evaluation*. Oxford University Press,
17 NY, NY, 483 pp.
- 18 -Herrera-Solaz, V., J. Segurado, J. Llorca (2015). On the robustness of an inverse optimization
19 approach based on the Levenberg–Marquardt method for the mechanical behavior of
20 polycrystals. *European Journal of Mechanics - A/Solids* 53, 220-228.
- 21 -Hu, L.Y. (2000). Gradual deformation and iterative calibration of gaussian-related stochastic
22 models. *Mathematical Geology* 32 (1), 87–108.
- 23 -Ignacio, I. (2014). Different ways to consider heterogeneity in quasi-fragile materials using a
24 version of lattice model. *Procedia Materials Science* 3, 499 – 504.
- 25 -Khan, M., Srivastava, S., Gupta, M.K. (2019). Hybrid wood particulates composites: mechanical
26 and thermal properties. *Materials Research Express* 6(10), 105323. DOI: 10.1088/2053-
27 1591/ab3835.
- 28 -Kashfi, M., Majzoubi, G.H., Bonora, N., Iannitti, G., Ruggiero, A., Khademi, E. (2018). A New
29 Overall Nonlinear Damage Model for Fiber Metal Laminates Based on Continuum Damage
30 Mechanics. *Engineering Fracture Mechanics*. 206, 21-33. DOI:
31 10.1016/j.engfracmech.2018.11.043.
- 32 -Kashfi, M., Majzoubi, G.H., Bonora, N., Iannitti, G., Ruggiero, A., Khademi, E. (2017). A study on
33 fiber metal laminates by using a new damage model for composite layer. *International Journal*
34 *of Mechanical Sciences* 131–132, 75-80. DOI: 10.1016/j.ijmecsci.2017.06.045.
- 35 - Kim, H., Kim, D., Ahn, K. (2015). Inverse Characterization Method for Mechanical Properties of
36 Strain/Strain-Rate/Temperature/Temperature-History Dependent Steel Sheets and Its
37 Application for Hot Press Forming. *Metals and Materials International* 21(5), 874-890.
- 38 -Kouznetsova, V., W. A. M. Brekelmans, F. P. T. Baaijens (2001). An approach to micro-macro
39 modeling of heterogeneous materials. *Computational Mechanics* 27, 37-48.
- 40 -Li, G., F. Xu, G. Sun, Q. Li (2014). Identification of mechanical properties of the weld line by
41 combining 3D digital image correlation with inverse modelling procedure. *International Journal*
42 *of Advanced Manufacturing Technology* 74, 893–905.
- 43 -Libanori, R., Erb, R.M., Reiser, A., Ferrand, H.L., Süess, M.J., Spolenak, R., Studart, A.R. (2012).
44 Stretchable heterogeneous composites with extreme mechanical gradients. *Nature*
45 *Communications* 3, 1265.
- 46 -Lloyd, A. A., Z. X. Wang, E. Donnelly (2015). Multiscale Contribution of Bone Tissue Material
47 Property Heterogeneity to Trabecular Bone Mechanical Behavior. *Journal of Biomechanical*
48 *Engineering* 137(1), 010801.
- 49 -Majzoubi, G.H., Kashfi, M., Bonora, N., Iannitti, G., Ruggiero, A., Khademi, E. (2018). Damage
50 characterization of aluminum 2024 thin sheet for different stress triaxialities. *Archives of Civil*
51 *and Mechanical Engineering* 18(3), 702-712. DOI: 10.1016/j.acme.2017.11.003.
- 52 -Mehrez, L., A. Doostan, D. Moens, D. Vandepitte (2012). Stochastic identification of composite
53 material properties from limited experimental databases, Part II: Uncertainty modelling.
54 *Mechanical Systems and Signal Processing* 27, 484–498.
- 55
56
57
58
59
60

- 1
2
3 -Mehrez, L., D. Moens, D. Vandepitte (2012). Stochastic identification of composite material
4 properties from limited experimental databases, Part I: Experimental database construction.
5 *Mechanical Systems and Signal Processing* 27, 471–483.
- 6 -Mikdam, A., A. Makradi, Y. Koutsawa, S. Belouettar (2013). Microstructure effect on the
7 mechanical properties of heterogeneous composite materials. *Composites: Part B* 44, 714–721.
- 8 -Mortazavi, F., E. Ghossein, M. Lévesque, I. Villemure (2014). High resolution measurement of
9 internal full-field displacements and strains using global spectral digital volume correlation.
10 *Optics and Lasers in Engineering* 55, 44–52.
- 11 -Ni, Y., M. Y.M. Chiang (2007). Prediction of elastic properties of heterogeneous materials with
12 complex microstructures. *Journal of the Mechanics and Physics of Solids* 55, 517–532.
- 13 -Pitangueira, R.L., R. R. Silva (2002). Numerical Characterization of Concrete Heterogeneity.
14 *Materials Research* 5, 309-314.
- 15 -Oller, S., Miquel, J., Zalamea, F. (2005). Composite material behavior using a homogenization
16 double scale method. *Journal of Engineering Mechanics*, 131(1), 65-79.
- 17 -Pottier, T., F. Toussaint, P. Vacher (2011). Contribution of heterogeneous strain field
18 measurements and boundary conditions modelling in inverse identification of material
19 parameters. *European Journal of Mechanics - A/Solids* 30(3), 373-382.
- 20 -Rahmani, B., F. Mortazavi, I. Villemure, M. Levesque (2013). A new approach to inverse
21 identification of mechanical properties of composite materials: Regularized model updating.
22 *Composite Structures* 105, 116–125.
- 23 -Saabye-Ottosen, N., Ristinmaa, M. (2005). *The Mechanics of Constitutive Modeling*. Elsevier
24 Ltd, 700 pages. ISBN 978-0-08-044606-6. DOI: 10.1016/B978-0-08-044606-6.X5000-0
- 25 -Sakata, S., F. Ashida, M. Zako (2008). Kriging-based approximate stochastic homogenization
26 analysis for composite materials. *Computer Methods in Applied Mechanics and Engineering* 197
27 (21–24), 1953–1964.
- 28 -Samavati, N., D. M. Mc Grath, M. A.S. Jewett, T. van der Kwast, C. Ménard, K. K. Brock (2015).
29 Effect of Material Property Heterogeneity on Biomechanical Modeling of Prostate under
30 Deformation. *Physics in Medicine & Biology*, 60(1), 195–209.
- 31 -Sánchez-Palencia, E. (1987). *Homogenization techniques for composite media*. Springer-Verlag,
32 Berlin, Germany.
- 33 -Sharifi, H., D. Larouche (2014). Numerical Study of Variation of Mechanical
34 Properties of a Binary Aluminum Alloy with Respect to Its Grain Shapes. *Materials* 7, 3065-3083.
- 35 -Sriramula, S., M. K. Chryssanthopoulos (2009). Quantification of uncertainty modelling in
36 stochastic analysis of FRP composites. *Composites Part A: Applied Science and Manufacturing*
37 40(11), 1673–1684.
- 38 -Torquato, S. (2010). Optimal Design of Heterogeneous Materials. *Annual Review of Materials*
39 *Research* 40:101-129.
- 40 -Ying, Z., J.J. Gómez-Hernández (2000). An improved deformation algorithm for automatic
41 history matching. Report 13, Stanford Center for Reservoir Forecasting (SCRF) Annual Report,
42 Stanford, CA.
- 43 -Wu, X., Y. Zhu (2017). Heterogeneous materials: a new class of materials with unprecedented
44 mechanical properties. *Materials Research Letters* 5:8, 527-532.
- 45 -Zhang, Z., C. Zhan, K. Shankar, E.V. Morozov, H. Kumar, T. Ray (2017). Sensitivity analysis of
46 inverse algorithms for damage detection in composites. *Composite Structures* 176, 844-859.
- 47 -Zottis, J., Theis, C.A., da Silva, A (2018). Evaluation of experimentally observed asymmetric
48 distributions of hardness, strain and residual stress in cold drawn bars by FEM-simulation.
49 *Journal of Materials Research and Technology*. DOI: 10.1016/j.jmrt.2018.01.004.
- 50
51
52
53
54
55
56
57
58
59
60

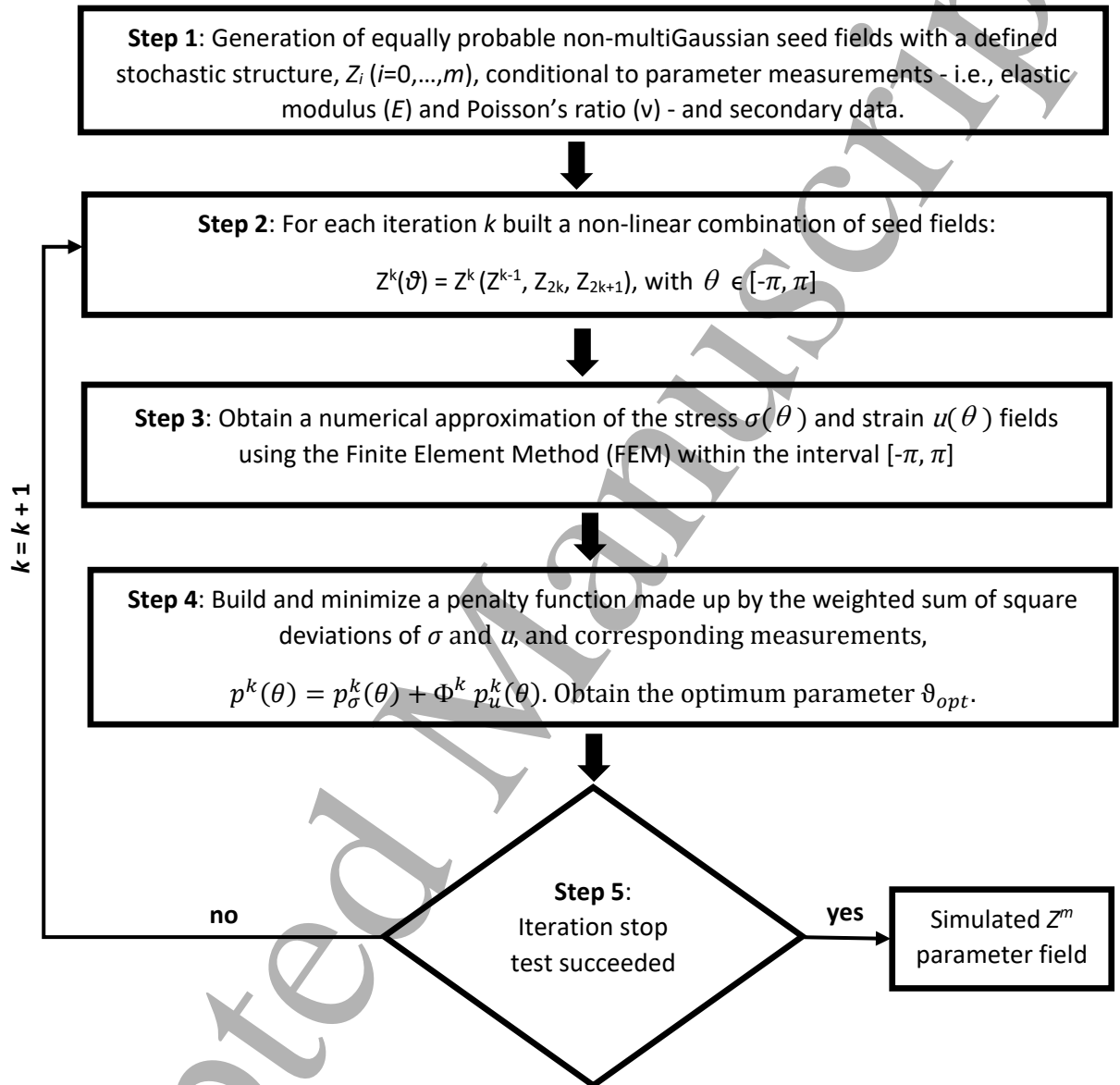


Fig. 1. Flowchart of the methodology.

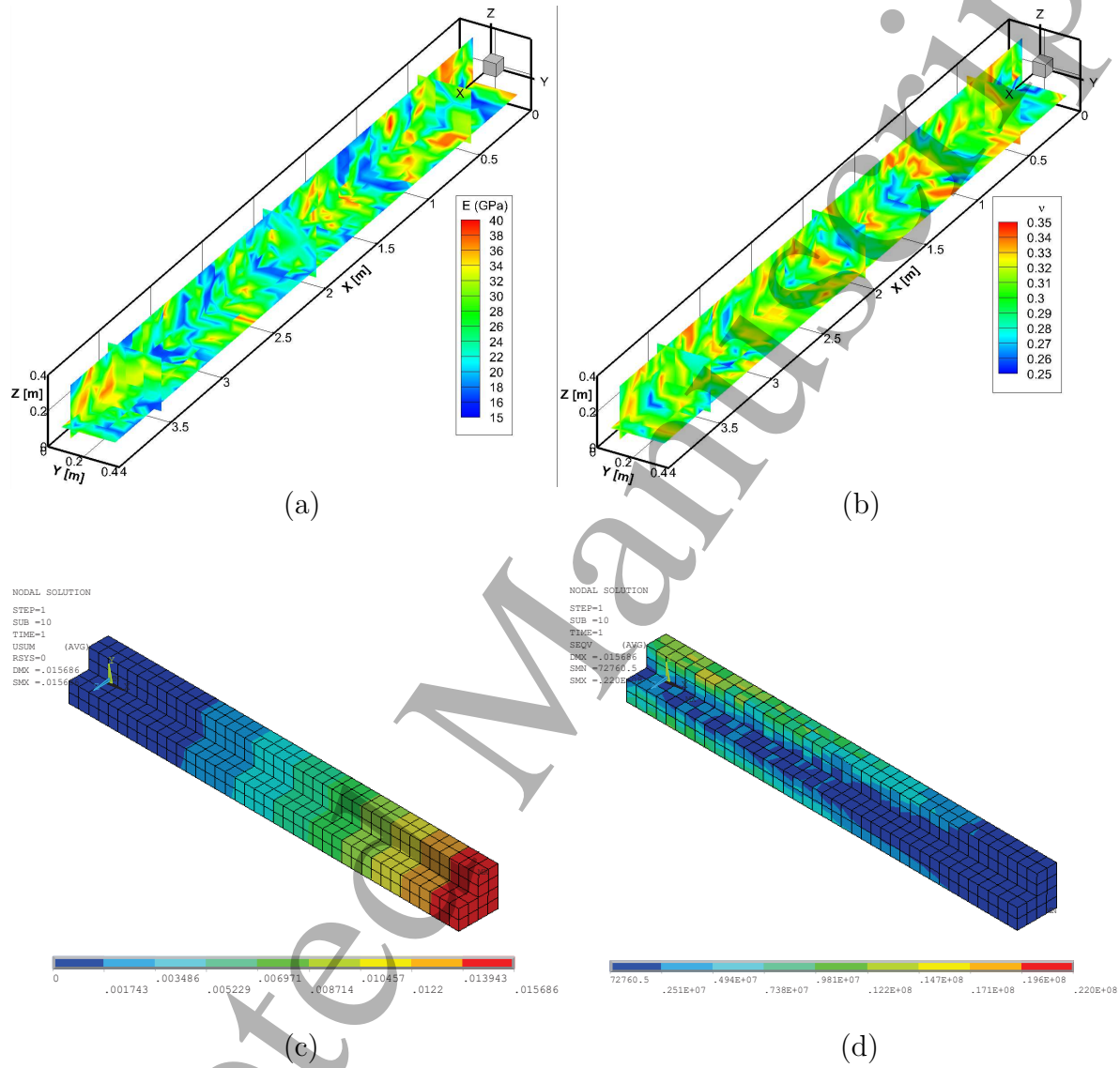


Fig. 2. Effective material property parameters for the reference field.

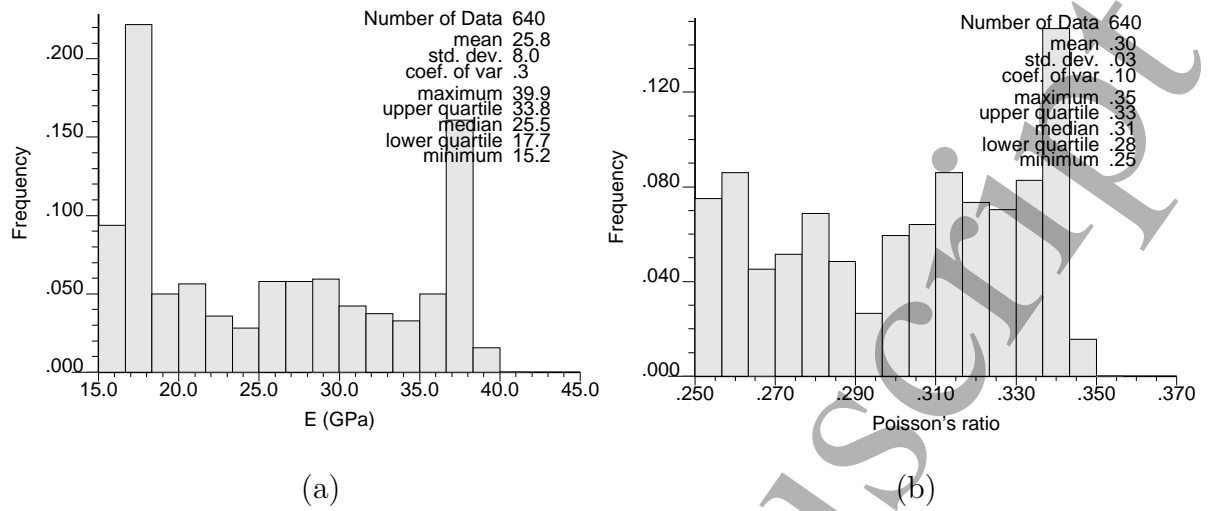


Fig. 3. Frequency distribution and the univariate statistics for the material property parameters (elastic modulus and Poisson's ratio values) of the reference field.

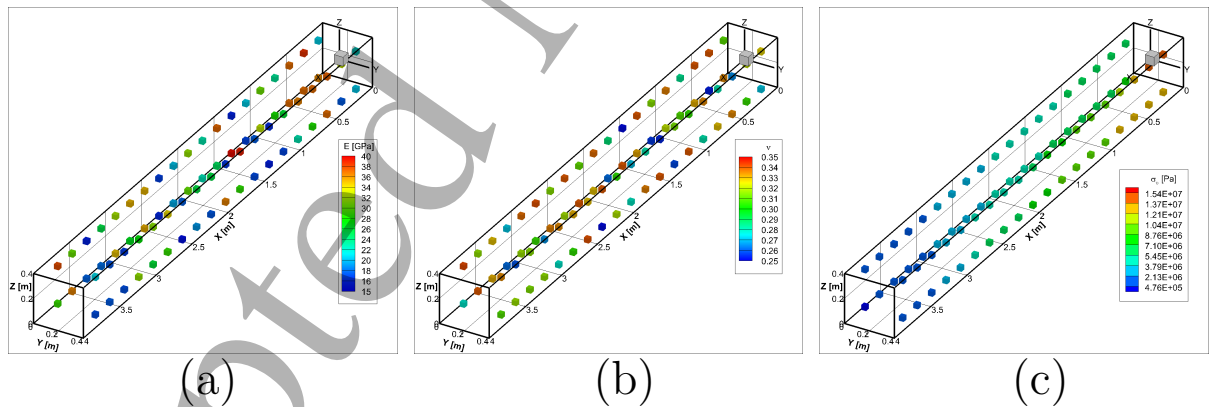


Fig. 4. Spatial location of conditioning data with regard to the elastic modulus (a), the Poisson's ratio (b) and the stress field (c).

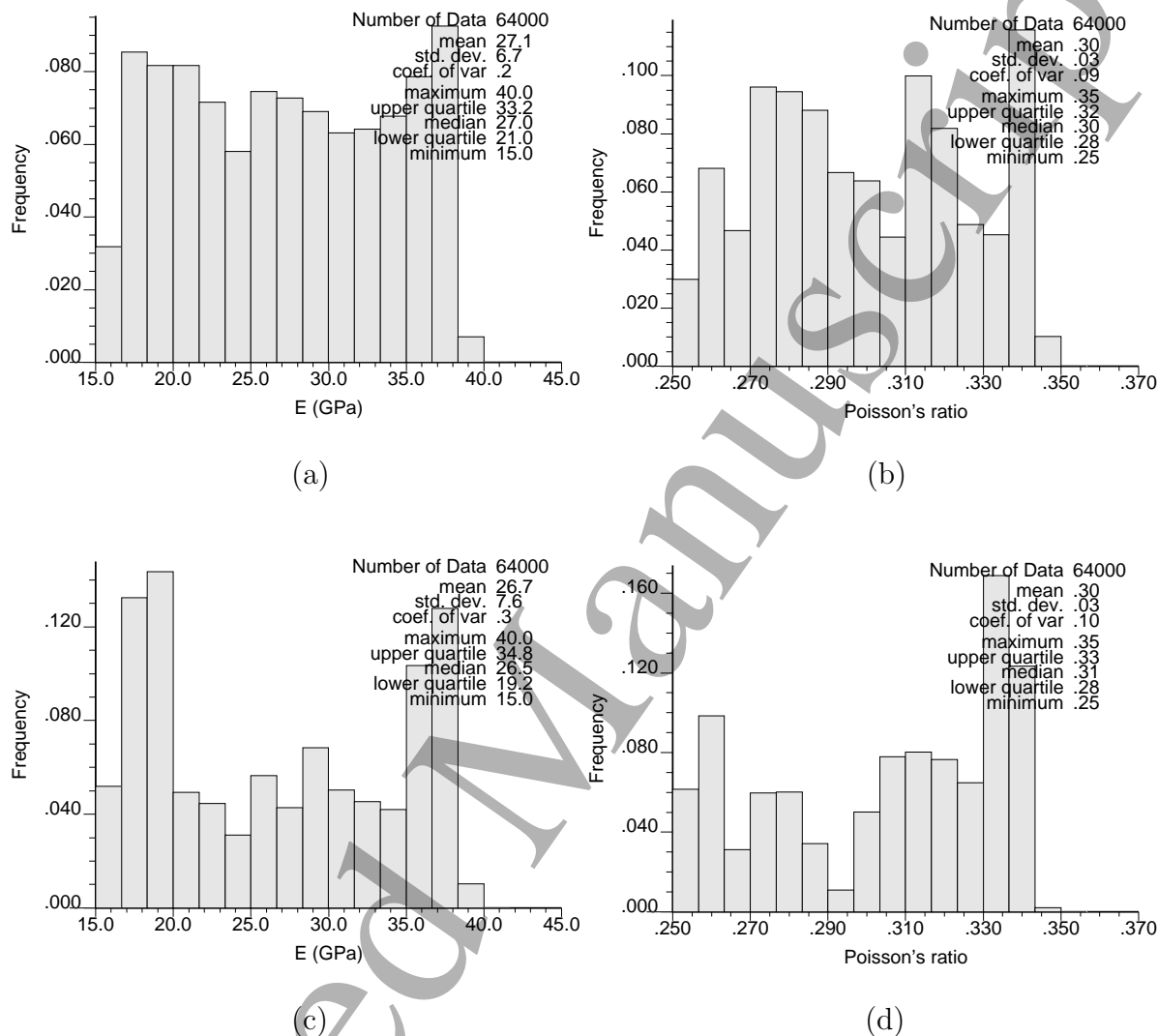


Fig. 5. Frequency distribution and the univariate statistics for an ensemble of a hundred fields of both unconditional (a: elastic modulus and b: Poisson's ratio) and conditional fields (c: elastic modulus and d: Poisson's ratio).

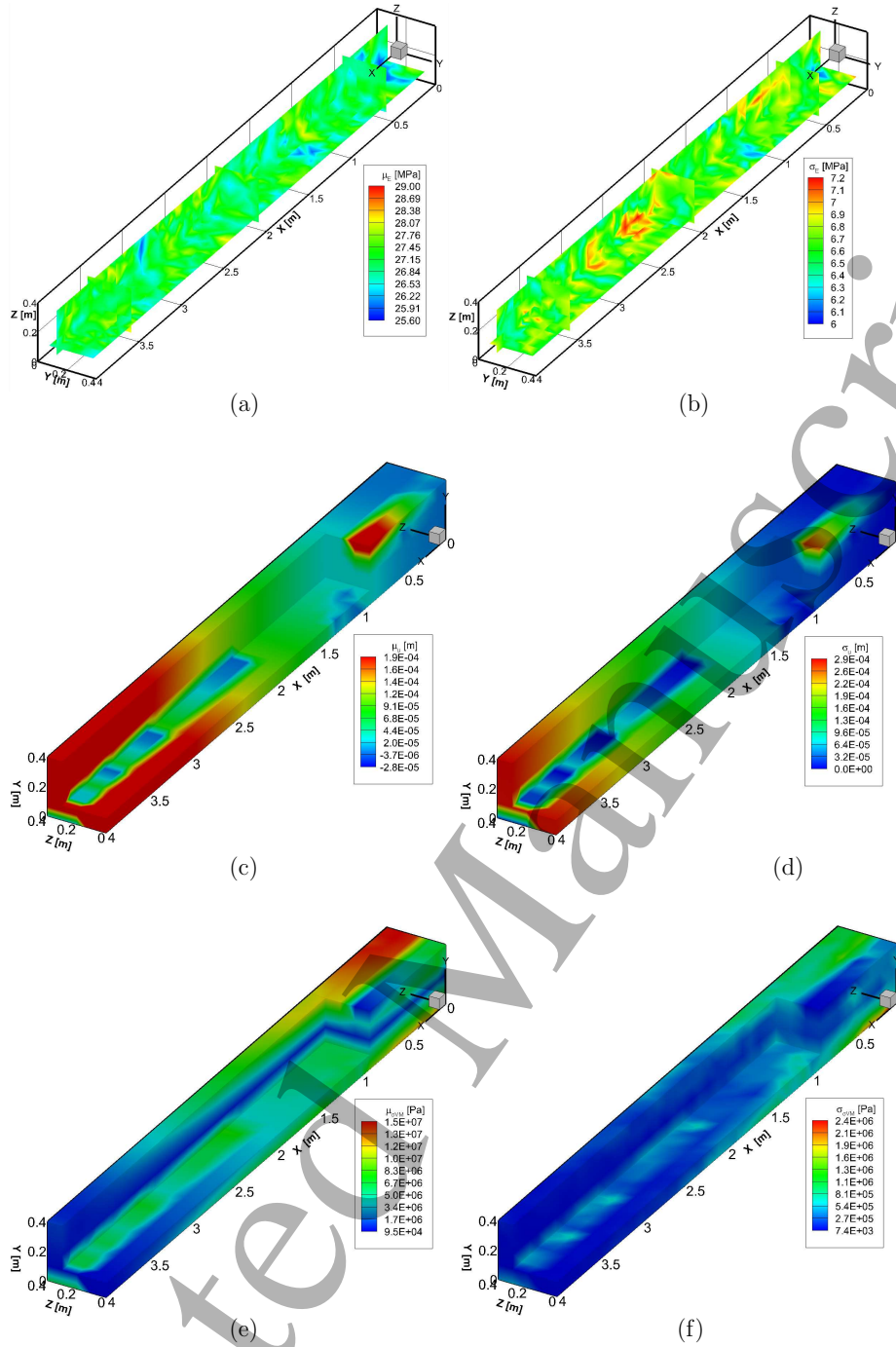


Fig. 6. Ensemble mean (μ) and standard deviation (σ) fields for a hundred unconditional realizations: (a) ensemble mean of the elastic modulus field (μ_E), (b) ensemble standard deviation of the elastic modulus field (σ_E), (c) ensemble mean of the displacement field (μ_u), (d) ensemble standard deviation of the displacement field (σ_u), (e) ensemble mean of the von Mises stress field ($\mu_{\sigma_{VM}}$), (f) ensemble standard deviation of the von Mises stress field ($\sigma_{\sigma_{VM}}$).

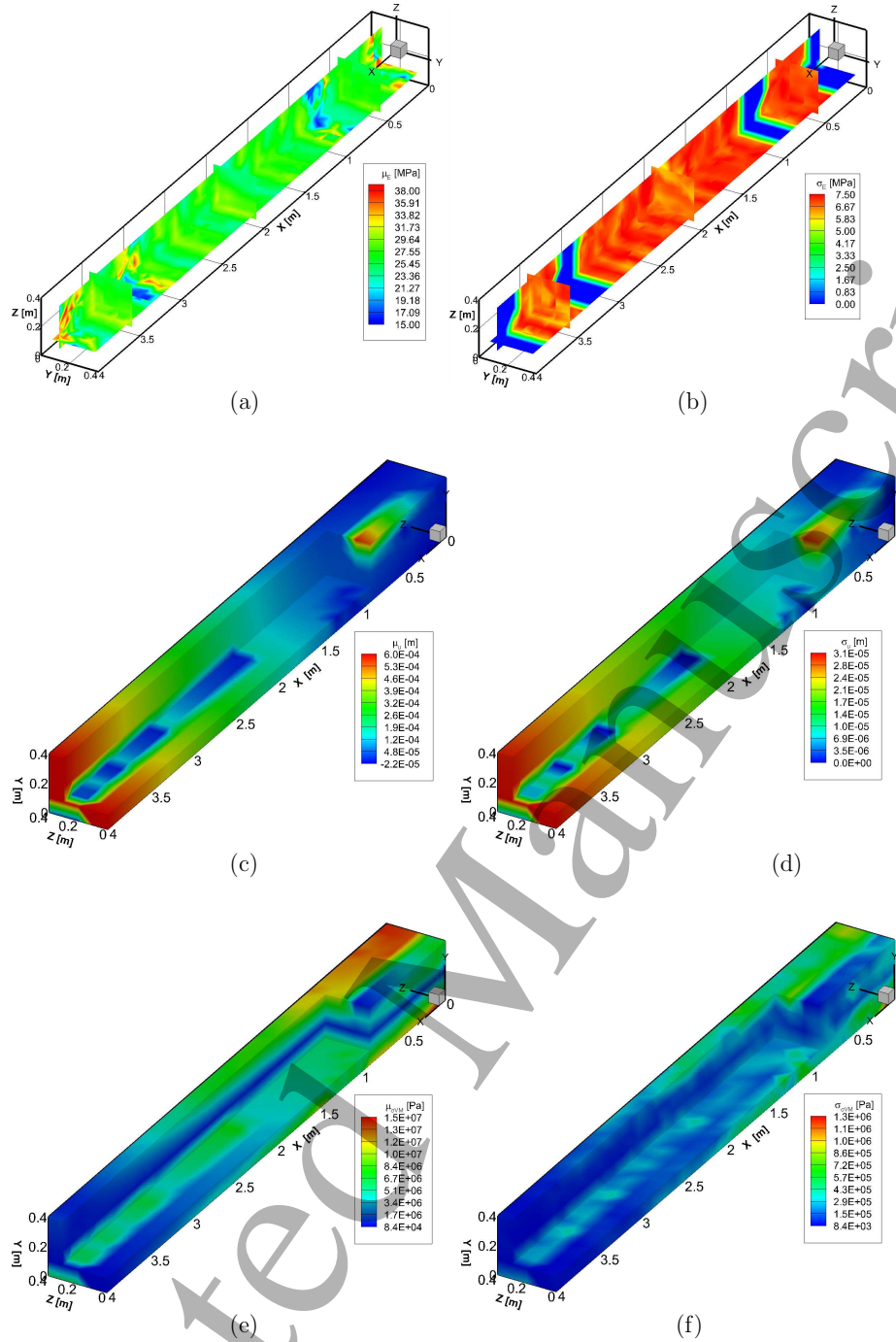


Fig. 7. Ensemble mean (μ) and standard deviation (σ) fields for a hundred conditional realizations: (a) ensemble mean of the elastic modulus field (μ_E), (b) ensemble standard deviation of the elastic modulus field (σ_E), (c) ensemble mean of the displacement field (μ_u), (d) ensemble standard deviation of the displacement field (σ_u), (e) ensemble mean of the von Mises stress field ($\mu_{\sigma_{VM}}$), (f) ensemble standard deviation of the von Mises stress field ($\sigma_{\sigma_{VM}}$).

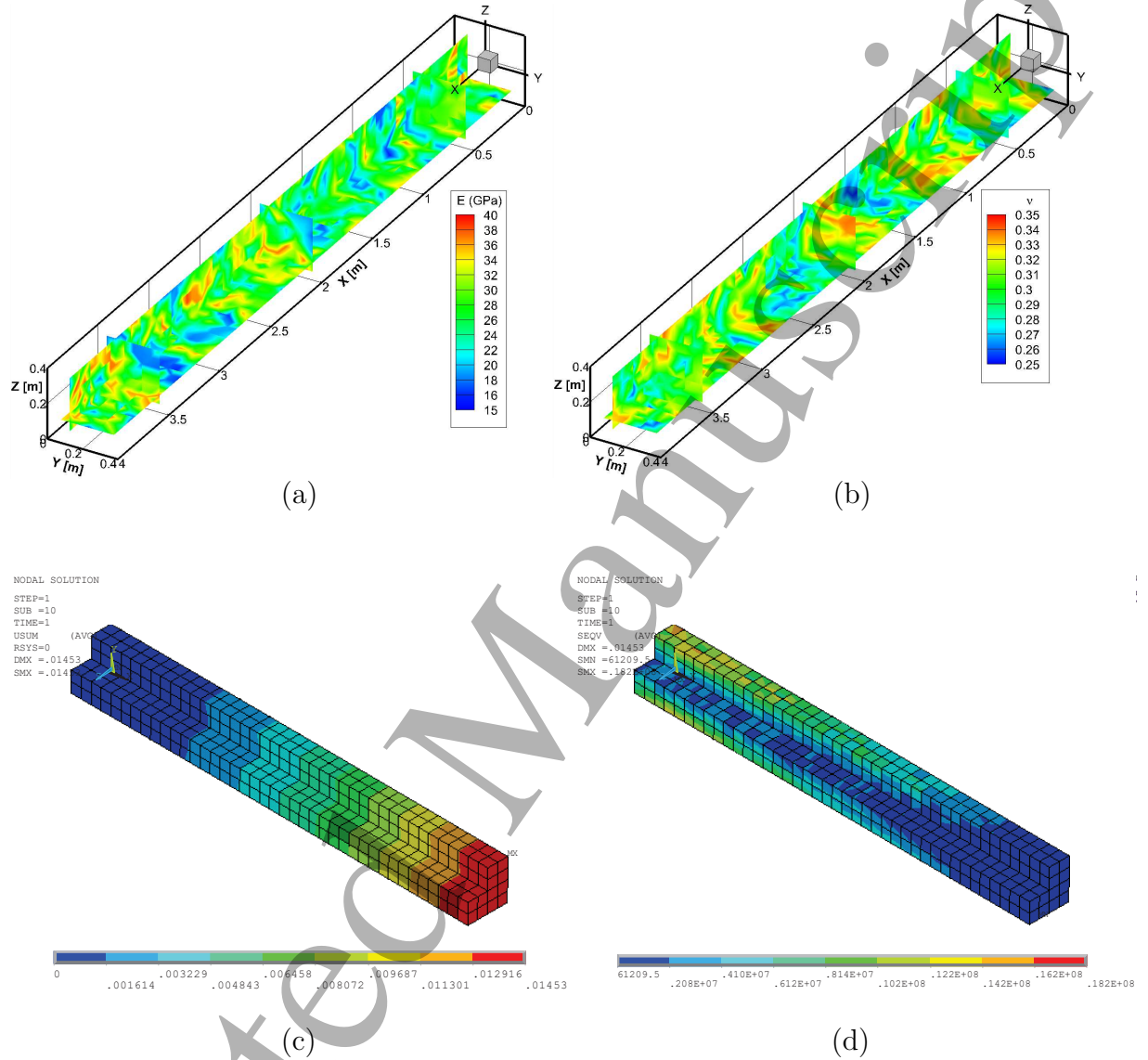


Fig. 8. Material property fields for a given conditional realization: elastic modulus (a), Poisson's ratio (b); and its corresponding displacement (c) and stress fields (d).

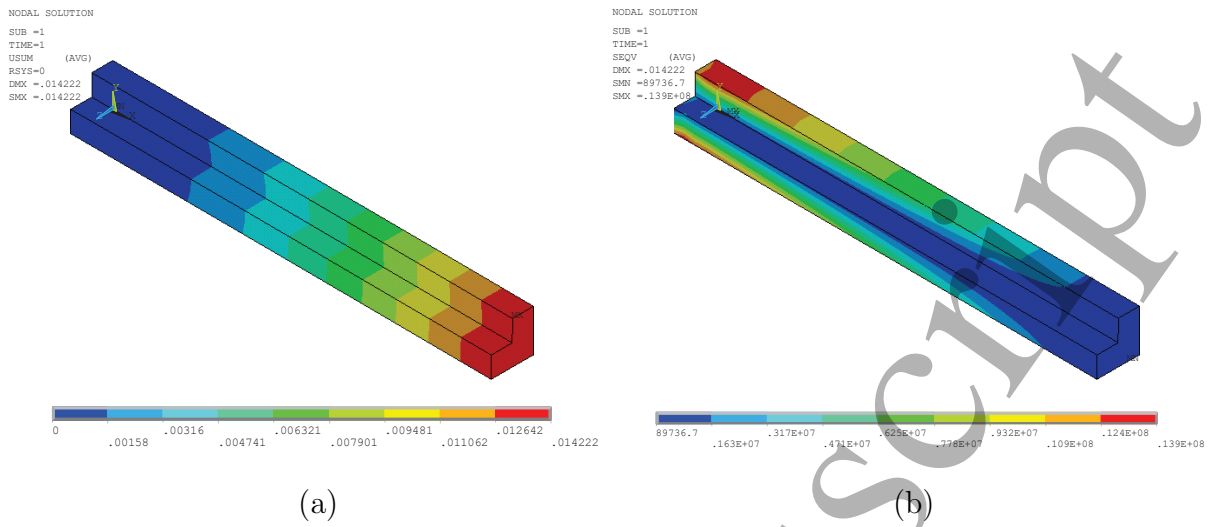


Fig. 9. Displacement (a) and stress (b) fields for and homogeneous material properties realization.

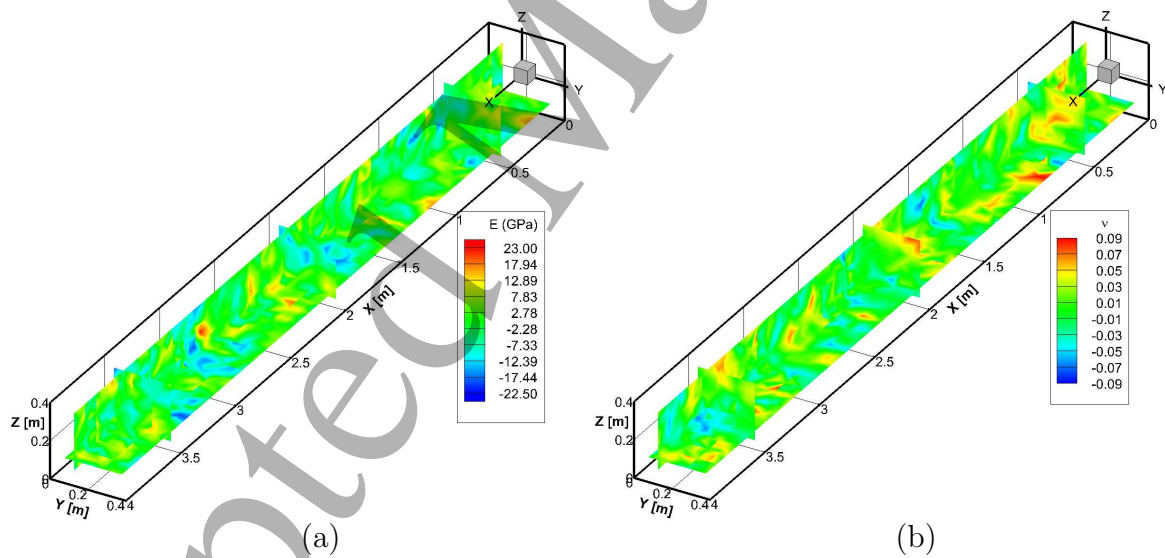


Fig. 10. Deformation field for a given realization, i.e., the field of optimal increments added to a certain unconditional parameter field at each element of the discretization for obtaining a conditional simulation.